

Design of Efficient Photonic Sensors Based on Vernier Effect in near-IR

B. Troia *, V. M. N. Passaro, F. De Leonardis
 Photonics Research Group, * CNIT UdR Bari
 Dipartimento di Elettrotecnica ed Elettronica
 Politecnico di Bari
 Via Edoardo Orabona n. 4, 70125 Bari - Italy
 E-mail: passaro@deemail.poliba.it
 URL: <http://dee.poliba.it/photonicsgroup>

A. V. Tsarev
 Laboratory of Optical Materials and Structures
 A.V. Rzhanov Institute of Semiconductor Physics
 Siberian Branch of Russian Academy of Sciences
 Novosibirsk, 630090, Russia
 E-mail: tsarev@isp.nsc.ru

Abstract— Integrated architectures based on cascaded ring resonators through the Vernier effect have been theoretically investigated and optimized for sensing applications. Sensitivity higher than 100 $\mu\text{m}/\text{RIU}$ allows detection of lead Pb(II) in water (< 50 ppb) and m-xylene gas (< 60 ppm) to be achieved, exhibiting limits of detection as low as 3.5×10^{-6} RIU.

Keywords—Group IV Photonics; Homogeneous optical sensing; Silicon-on-Insulator; Vernier effect;

I. INTRODUCTION

Photonic sensors have been the subject of intensive research over the last two decades. Interesting applications have been experimentally demonstrated for chemical, biochemical and gas sensing, to name a few. In this paper, photonic sensors based on cascaded ring resonator (RR) configuration and operating in the second regime of Vernier effect [1-2], are theoretically investigated, evaluating design and performance. Modal propagation has been simulated in wire optical waveguides based on CMOS-compatible silicon-on-insulator (SOI) technology. These photonic devices have been already integrated in MZI configurations and fabricated [3] for detection of lead contaminant of water, e.g. BTEX compounds (benzene, toluene, ethylbenzene, xylene) and volatile organic compounds (VOCs) in air. Theoretical results have been compared with experimental measurements in literature [3], demonstrating ultra high performance of cascaded RR photonic sensors based on the Vernier effect.

II. ARCHITECTURES OF PHOTONIC SENSORS BASED ON VERNIER EFFECT

Photonic sensors considered in this investigation are constituted by two cascaded RRs, as sketched in Fig. 1. In particular, the first RR, with perimeter length L_{filter} , acts as a filter, while the second one (perimeter length L_{sensor}) acts as a sensor, being directly exposed to the cover medium. The whole architecture is covered by an insulating thick cladding (e.g., SiO_2 , SU-8, teflon), with the only exception of a window opened on the sensing RR, where the test sample to be detected is concentrated. According to MZI configuration [3], the waveguide selected in this investigation is a silicon photonic wire, with height of 260 nm and width of 450 nm.

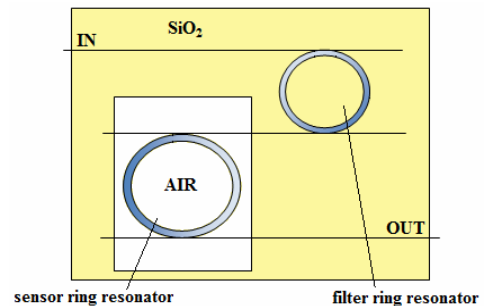


Figure 1. Architectural scheme of an integrated photonic sensor based on Vernier-effect in SOI technology, using a SiO_2 insulating cladding.

Four design configurations have been simulated for m-xylene and lead Pb (II) detection. The first one, named *Sensor 1*, is characterized by SU-8 insulating 2- μm -thick cladding with sensing RR directly exposed to air. The second architecture (*Sensor 2*) is similar to the previous one, with SiO_2 2- μm -thick layer insulating cladding. *Sensor 3* has been assumed by coating the same structure as *Sensor 1* with a micro-extraction polydimethylsiloxane (PDMS) film, 3.5 μm -thick. Finally, the last sensor configuration *Sensor 4* has been assumed by coating the chip *Sensor 2* with a micro-extraction film (400 nm-thick) based on a tetrasulfide-functionalized mesoporous silicate material.

A sophisticated algorithmic procedure has been implemented for design of these sensing architectures based on Vernier effect, by setting the operative wavelength $\lambda_{\text{sensor}} = 1529.4$ nm and propagation loss coefficient $\alpha = 1$ dB/cm. Finally, optimal filter and sensing RR perimeter lengths and differences among filter and sensor free spectral ranges (FSRs) have been found, as listed in Table I.

TABLE I. FILTER AND SENSING RR PERIMETER LENGTHS AND ΔFSR CALCULATED FOR VARIOUS SENSOR ARCHITECTURES

Architecture	L_{filter} (μm)	L_{sensor} (μm)	ΔFSR (pm)
<i>Sensor 1</i>	1403.85	1542.90	1.589
<i>Sensor 2</i>	1458.90	1589.25	1.497
<i>Sensor 3</i>	1812.20	1871.75	1.194
<i>Sensor 4</i>	1713.25	1824.10	0.815

Silicon photonic wire modal behavior has been investigated by full-vectorial 2D finite element method (FEM). In FEM mesh generation for effective indices and modal profile calculations, about 50,000 triangular vector-elements have been adopted. Finally, the thickness of the buried oxide is always set to 2 μm , being the top silicon layer 260 nm thick.

III. SENSING PERFORMANCE AND SIMULATIONS

Sensing performance of designed configurations are listed in Table II for each sensing architecture.

TABLE II. PERFORMANCE PARAMETERS OF VARIOUS SENSOR CONFIGURATIONS

Parameters	Sensor 1	Sensor 2	Sensor 3	Sensor 4
$\Delta\lambda_{peak}$ (nm)	1.1573	1.1919	1.4974	1.8236
$\Delta n_{c,min} \times 10^6$	6.7423	6.3552	4.0403	3.5373
$\Delta n_{c,max} \times 10^3$	3.3	3.2	2.0	2.8
$\Delta n_{eff,min} \times 10^6$	2.0227	1.9066	1.6161	1.0612
$S_2 \mu\text{m}/\text{RIU}$	115.73	119.19	149.74	182.36

^{*}induced by $\Delta n_c = 1 \times 10^{-5}$ RIU (refractive index unit)

Resonance wavelength shifts $\Delta\lambda_{peak}$, wavelength sensitivities S_2 , minimum $\Delta n_{c,min}$, maximum $\Delta n_{c,max}$ detectable cover refractive index (RI) changes and minimum detectable effective RI changes $\Delta n_{eff,min}$, have been considered and calculated in our automatic procedure. In Fig. 2 it is possible to observe dynamic ranges (DRs) for various sensor configurations. Wavelength shifts of Vernier peak $\Delta\lambda_{peak}$ have been simulated as a function of different cover refractive index changes, Δn_c , being the Vernier peak at $\lambda_{sensor} = 1529.4$ nm, when sensors operate at rest (absence of test sample from sensible area, $\Delta n_c = 0$). Consequently, when a cover RI change higher than the detectable one $\Delta n_{c,min}$ occurs, a wavelength shift $\Delta\lambda_{peak}$ affects the Vernier overall transmittance. *Sensor 3* and *Sensor 4* have been simulated for m-xylene and lead Pb(II) detection, respectively, considering the PDMS RI change upon xylene ($dn_{PDMS}/dC_{xylene} = 8.7 \times 10^{-7}$ RIU/ppm) and the mesoporous silica (MS) RI change upon lead Pb(II) ($dn_{MS}/dC_{Pb(II)} = 1.0-5.0 \times 10^{-6}$ RIU/ppb).

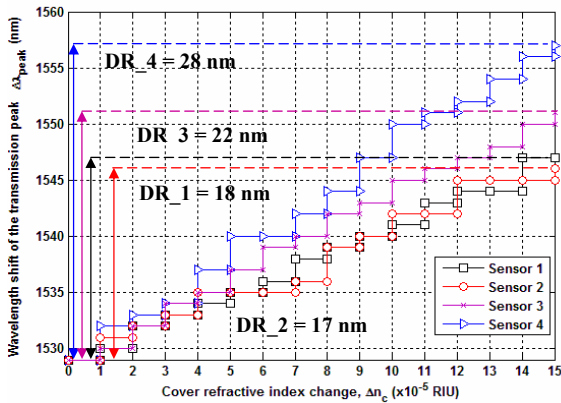


Figure 2. Wavelength shift $\Delta\lambda_{peak}$ versus cover RI change, $\Delta n_c \sim 10^{-5}$ RIU, for various selected sensing architectures.

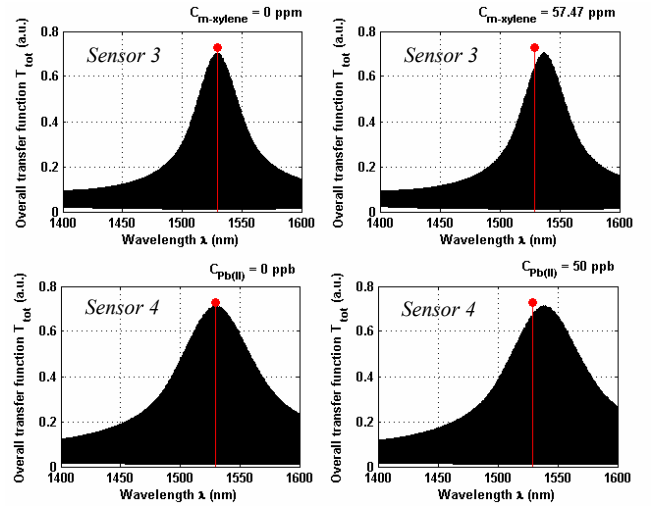


Figure 3. Simulations of *Sensor 3* and *Sensor 4* operation for m-xylene and lead Pb(II) detection. Red line is set at $\lambda_{sensor} = 1529.4$ nm.

Our results theoretically confirm *Sensor 3* as the best configuration for m-xylene gas detection using a PDMS cladding film, as in [3]. In fact, in Fig. 3 a m-xylene gas concentration as low as 57.47 ppm can be easily detected, being the relative wavelength shift as long as $\Delta\lambda_{peak} = 8$ nm. The configuration *Sensor 4* exhibits interesting performance for Pb(II) detection in water. In fact, by considering $dn_{MS}/dC_{Pb(II)} = 1.0 \times 10^{-6}$ RIU/ppb, a lead concentration as low as 50 ppb generates a wavelength shift $\Delta\lambda_{peak} = 11$ nm, revealing an ultra high sensing resolution (see Fig. 3). In conclusion, Table III shows a comparison between experimental results [3] through MZI-based sensors and theoretical results calculated in this paper using a Vernier-based approach. The latter shows clear sensing advantages.

TABLE III. COMPARISON BETWEEN VERNIER AND MZI CONFIGURATIONS BASED ON SILICON PHOTONIC WIRE WAVEGUIDES

Performance	Vernier [this paper]	MZI [3]
Sensor 3 – m-xylene detection		
Sensitivity	149.74 $\mu\text{m}/\text{RIU}$	4930 rad/RIU
Resolution	< 60 ppm	< 100 ppm
LOD	4.0403×10^{-6} RIU	0.43 rad
Sensor 4 – Pb(II) detection in water		
Sensitivity	182.36 $\mu\text{m}/\text{RIU}$	2536 rad/RIU
Resolution	< 50 ppb	100 ppb
LOD	3.5373×10^{-6} RIU	0.3 – 1.3 rad

REFERENCES

- [1] J. Hu and D. Dai, "Cascaded-Ring Optical Sensor With Enhanced Sensitivity by Using Suspended Si-Nanowires," *IEEE Photon. Tech. Lett.*, vol. 23, n. 13, pp. 842-844 (2011).
- [2] L. Jin, M. Li, J-J. He, "Highly-sensitive silicon-on-insulator sensor based on two cascade micro-ring resonators with Vernier effect," *Opt. Commun.*, vol. 284, n. 1, pp. 156-159 (2011).
- [3] J. Saunders, M. A. Dreher, J. A. Barnes, C. M. Crudden, J. Du, H. Loock, *et al.*, "Detection of lead contamination of water and VOC contamination of air using SOI micro-optical devices," *Conf. Proc. of 7th IEEE Group IV Photon. (GFP)*, pp. 177-179, 1-3 Sept. 2010.